Processing of Velocity Observations from Ice-Tethered Profilers

Sylvia T. Cole, Fredrick T. Thwaites, Richard A. Krishfield, and John M. Toole
Woods Hole Oceanographic Institution, Woods Hole, Massachusetts 02543
Email: scole@whoi.edu

***Abstract*—Ocean velocity in the Arctic is estimated using a three-axis acoustic travel-time current meter onboard an Ice-Tethered Profiler (ITP). The ITP is moored on an ice floe, with the current meter measuring velocity past the sensor as it profiles vertically through the water column along an inclined wire and translates horizontally with the motion of the overlying sea ice. Accurate estimates of ocean velocity rely on simultaneous estimates of instrument pitch, roll, and heading, the velocity at which the sensor crawls along the wire, and the velocity of the overlying sea ice. An inertial measurement unit is used to derive instrument pitch, roll, and heading from a three-axis flux-gate compass, accelerometer, and angle rate gyro. Instrument speed along the wire is derived from pressure as measured by the CTD. Hourly GPS fixes of the surface package are used to estimate ice velocity. Pre-deployment calibrations are preformed to determine magnetometer, accelerometer, pitch, roll, and heading biases. Post-deployment calibration parameters are determined to account for remaining biases. Post-deployment parameters are chosen so that there is no obvious bias related to wire angle, velocity estimates when the profiler is stationary versus moving, or upward versus downward profiles. These procedures are described as implemented for the second-generation velocity sensor deployed in the Arctic Ocean on five Ice-Tethered Profilers during 2013-2015.**

I. Introduction

Arctic Ocean currents are difficult to measure due to their weak strength, low backscatter levels, and the overlying ice cover. Ice-Tethered Profilers with Velocity (ITP-Vs) use an acoustic travel-time current meter that does not rely on backscatter, and a platform tethered on and drifting with an ice floe. Traveling with the ice allows measurements within a few meters of the ice-ocean interface without damage to the instrument. Data are available from the second-generation ITP-V on five systems (ITP 70, 77, 78, 79, and 80) that operated between 2013 and 2015 as part of ONR's Marginal Ice Zone program in the Canada Basin. This paper describes the processing of the velocity observations from these five systems.

The five ITP-Vs were deployed during three field campaigns within the Canada Basin (Fig. 1a). A pilot ITP-V (ITP 70) operated from August 2013 to July 2014 with sampling ending due to battery life. Three ITP-Vs (ITP 77, 78, and 79) were deployed from ice camps in the eastern Canada Basin in March 2014, and subsequently drifted westward as the surrounding ice cover melted. Data telemetry ceased on 6 August 2014 due to a software problem for ITP 78, and the other two systems (ITP 77 and ITP 79) were recovered in October 2014 by a ship of opportunity. ITP 80 collected data from August 2014 to May 2015. A total of 8,888 profiles and 3,840 fixed depth records were obtained over a total of 1,150 instrument-days of sampling. Profiles were obtained from 6 m below the ice-ocean interface to 250 or 750 m depth. Fixed depth records were collected a few meters beneath the ice-ocean interface and used to estimate the vertical turbulent fluxes of heat, salt, and momentum. The ITP-Vs sampled in a range of ice conditions from full ice cover to nearly open water conditions that corresponded to a range of wire angles and ocean velocity signals (e.g., internal wave energy levels), making this dataset highly suitable for determining appropriate velocity processing procedures.

This paper is organized as follows. Additional details of ITP-Vs are provided in Section II. The derivation of ocean velocity including quality control procedures, and pre-deployment and post-deployment calibration procedures are described in Section III. Section IV discusses the fixed depth records. Error in ocean velocity is discussed in Section V. A summary is provided in Section VI.

II. Overview of ITP-Vs

Ice-Tethered Profilers have been deployed in the Arctic Ocean since 2004 [1], [2]. ITPs consist of a surface buoy that includes satellite communication, a 750 m wire, a profiling package (McLane ITP) that crawls along the wire, and a weight at the bottom of the wire (Fig. 1b). ITPs typically profile twice per day to 750 m depth measuring temperature, salinity, and pressure. The upper 5 m of wire is reinforced to prevent damage during ice convergences, and so the uppermost measurement is typically at 6-8 m depth. CTD data are processed according to [3]. A surface package records GPS position every hour, from which ice velocity is derived (see Sect. III-B1). Each ITP typically lasts for one to several years drifting with the sea ice or in the open ocean if sea ice is not present. ITPs telemeter data in near-real time, and are considered expendable. ITP data and additional resources are available at http://www.whoi.edu/itp.

The five Marginal Ice Zone ITP-Vs constitute the initial deployment of the second-generation system. The first generation ITP-V consisted of a single system (ITP 35), which had noise at periods less than 10 s caused by one of the acoustic paths of the velocity sensor sampling the wake generated by its support structure [4], [5], [6]. The first generation ITP-V measured at 2 Hz with no averaging of instrument attitude at higher frequencies. The second-generation ITP-V includes a velocity

978-0-933957-43-5 ©2015 MTS

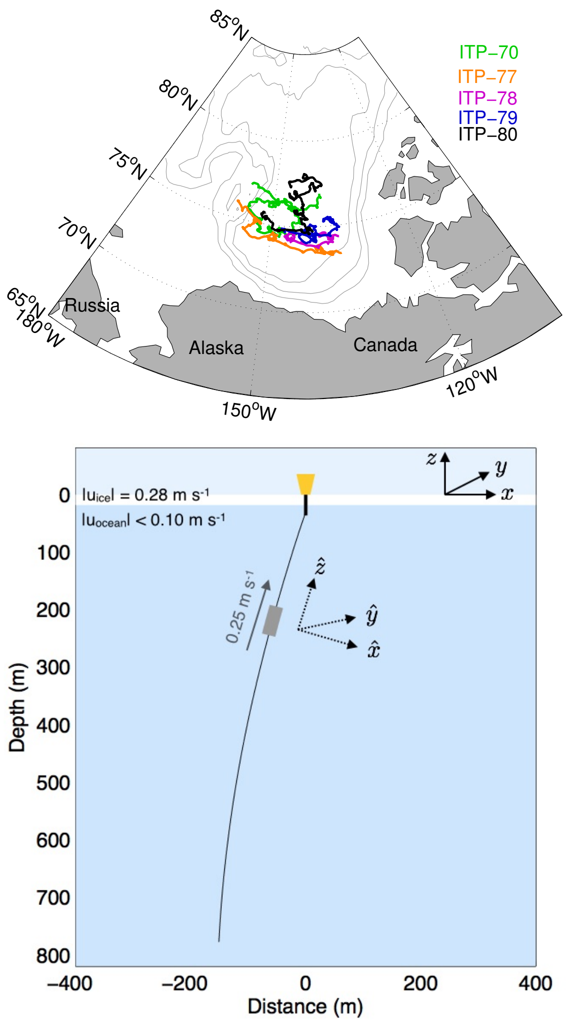

Fig. 1. a) Map of ITP-V locations. Drift tracks for each ITP-V system are shown in color. Contours show topography for 1000, 2000, and 3000 m depth. b) Schematic of an ITP-V showing the surface buoy (yellow), wire (black), and profiler package (gray). The geographic coordinate system (x,y,z; solid arrows) and sensor coordinate system ($\hat{x}$,$\hat{y}$,$\hat{z}$; dashed arrows) that is aligned with the MAVS are illustrated. The wire profile shown is from ITP 78 on 17 Jun 2014 with an average wire angle of 16° in the upper 250 m, ice velocity of 0.28 $m\ s^{-1}$, ocean velocities less than 0.10 $m\ s^{-1}$, and a satellite based ice concentration of 100%. Wire angle is to scale.

Fig. 2. a) ITP-V (ITP 78) during deployment through a hole in the ice. b) ITP-V profiler in the jig for pre-deployment spin tests. The MAVS is circled in red. Spin tests were performed outside on a pad designed to be free of magnetic anomalies.

sensor redesigned to minimize noise [4], [5], pre-deployment calibrations, and a different inertial measurement unit (IMU) to better estimate profiler attitude at high frequencies.

The ITP-V includes a velocity sensor, IMU, and fin to align the velocity sensor into the flow (Fig. 2). A Modular Acoustic Velocity Sensor (MAVS; [5], [7], and [8]) is used, and consists of four acoustic paths that measure travel time differences of acoustic signals sent between sets of transducer pairs surrounding a small volume of water bracketed by the transducer stings. The ITP-V is constrained to fit through a 0.6 m diameter hole for deployment, which necessitates the placement of the MAVS transducer array close to the profiler body. A fin aligns the MAVS into the flow, with profiler roll typically a fraction of pitch. Alignment into the flow is an attempt to ensure that any profiler wake is advected away behind the sensor. Since the MAVS is at the top of the profiler, a non-zero wire angle is advantageous to avoid wake effects when profiling downwards. The inertial measurement unit consists of integral three-axis fluxgate compass, accelerometer, and angle rate gyro sensors. The IMU measures at 200 Hz, integrates attitude estimates with a Kalman filter, and outputs to a 1 Hz record. Compared with the first generation ITP-V, noise in pitch, roll, and heading estimates are reduced, and data can be recorded at 1 Hz thereby reducing telemetry costs and increasing battery life.

The CTD and MAVS sensors are treated similarly by the ITP. At the start of each record, a controller turns on the power to the CTD and MAVS, which then boot up and begin recording. Because the boot up times differ, the CTD and MAVS do not start sampling at the same time. Data are

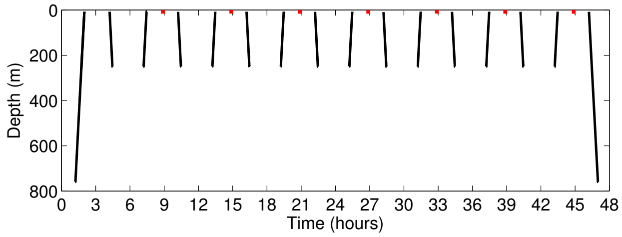

Fig. 3. Sampling pattern for ITP-Vs showing the two-day repeat pattern with profiles in black and fixed depth observations in red.

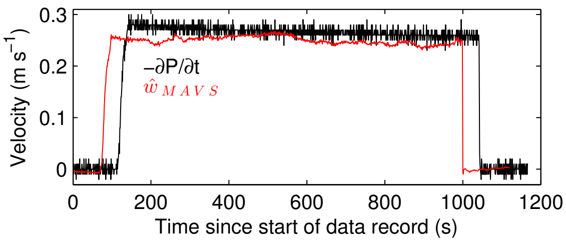

Fig. 4. Vertical velocity past the MAVS sensor ($\hat{w}_{MAVS}$; red), and the difference in CTD pressure (black) during a 250 m upward profile for ITP 78. The CTD starts recording data before the MAVS due to differences in the time it takes each sensor to boot up. The MAVS turns off before the CTD at the end of a record. The time stretching and offset factors align the two records. Note that vertical velocities do not exactly match do to the use of sensor and geographic coordinate systems.

obtained from the CTD and MAVS sensors every second. At the end of a record, data are offloaded to the controller, sent up to the surface package via an inductive modem, and sent to shore via an Iridium link.

For the observations described here, sampling consisted of profiles and fixed depth records (Fig. 3). One-way profiles between approximately 8 and 250 m depth were obtained every 3 hours, with two profiles per 48-hour period extending to 750 m depth. The three-hour time interval is chosen to capture near-inertial and tidal motions with periods near 12 hours. After each upward profile from 250 m depth, sampling at fixed depth just beneath the ice for a period of 24 minutes is performed. This allows the turbulent fluxes of heat, salt, and momentum to be directly estimated. For profiles, the profiler is programmed to begin moving after a period of two minutes, and to wait two minutes before turning off at the end of a profile (Fig. 4). The first and last 90 s are ultimately removed from the final product, but these stationary data aid in determining post-deployment calibration parameters in part by ensuring that velocity data are consistent whether the profiler is moving or not. For a typical speed along the wire of $0.25\ m\ s^{-1}$ (Fig. 4), 0.25 m vertical resolution is obtained. At high wire angle, corresponding roughly to ice speeds greater than $0.3\ m\ s^{-1}$ or wire angles greater than $15°$, the profiler can have difficulty climbing the wire. The profiler can also slip down the wire while waiting at the surface, resulting in a fixed depth record that is below 8 m depth, or a pressure change during the 20 minute fixed depth record. In addition, the minimum pressure for the start of the next down profile can be deeper still. Overall, only 2% of upward profiles did not reach 12 m, 5% of fixed depth records were deeper than 12 m, and 6% of downward profiles began deeper than 12 m. This sampling scheme corresponds to a one-year duration for the ITP-V; ITP 70, which was the only ITP-V to end its mission due to battery life, sampled for 324 days. Battery life is affected by the ice and ocean conditions during the deployment, which determine wire angle and so the energy needed to climb the wire.

III. Derivation of Ocean Velocity

The velocity sensor measures relative flow past the instrument. In the absence of ice or ocean currents, this flow results from the profiler moving along the wire, rotating around the wire, and translating horizontally due to ice motion. Ocean velocity is calculated as:

$$\mathbf{u_{ocean}} = \mathbf{u_{MAVS}} + \mathbf{u_{ang}} + \mathbf{u_{wire}} + \mathbf{u_{ice}} \tag{1a}$$

$$\hat{\mathbf{u}}_{MAVS} = (c^2 \Delta t / 2d) u_{scale} \tag{1b}$$

where $\mathbf{u}_{MAVS}$ is the velocity measured relative to the sensor, $\mathbf{u_{ang}}$ is the angular velocity due to rotation around the wire, $\mathbf{u_{wire}}$ is the velocity due to motion of the profiler along the inclined wire, $\mathbf{u_{ice}}$ is the horizontal ice velocity, c is sound speed, Δt is a travel time difference, d is the acoustic path length which is taken to be the shortest distance between transducer pairs, and u_{scale} is a magnitude correction that accounts for errors in the path length or travel time. The $\hat{x}$ notation indicates velocity in the coordinate system aligned with the MAVS sting; geographic coordinates are obtained after rotation by instrument pitch (θ), roll (ψ), and heading (ϕ) (Fig. 1b; Sect. III-B2). Sound speed is derived from observed temperature, salinity, and pressure. Since Arctic Ocean currents are frequently small, the horizontal velocity past the MAVS sensor is to a large degree equal and opposite to the ice velocity, with wire velocities becoming important at high wire angle (Fig. 5). For vertical velocity, the dominant balance is between the sensor and wire velocities. Overall, the ocean velocity, a small number, is derived by taking the difference between two large numbers. Thus, small errors in processing are important, but such errors are also largely possible to determine.

Velocity data are processed to 1) minimize dependence on wire angle, 2) ensure that ocean velocity estimates when the profiler is stationary agree with ocean velocity estimates when the profiler is moving, and 3) ensure that upward and downward profiles are not systematically biased. Nine calibration parameters are determined prior to deployment and account for biases in the magnetometer and accelerometer as well as any misalignment of the MAVS and IMU. Biases in the angle rate gyro measurements are not determined as the rate gyro measurements are only used when high-pass filtered, thereby reducing the effect of rate gyro biases. Seven calibration parameters are determined after deployment, and account for biases in heading, pitch, roll, and the overall magnitude of the velocity estimate, the radius at which the MAVS spins about the wire, as well as differences in timing between the velocity

TABLE I
SUMMARY OF CALIBRATION PARAMETERS

	ITP 70	ITP 77	ITP 78	ITP 79	ITP 80
Mx_{bias}	0.058	0.101	-0.326	0.126	-0.095
My_{bias}	-0.056	-0.026	-0.230	0.007	-0.054
Mz_{bias}	0.033	-0.018	0.232	-0.058	0.028
$Ax_{bias}(m^2s^{-1})$	-0.033	-0.015	0.026	-0.0.009	-0.010
$Ay_{bias}(m^2s^{-1})$	-0.139	0.001	0.019	-0.003	0.003
$Az_{bias}(m^2s^{-1})$	0.218	0.719	0.442	0.007	0.239
$\theta_{spin}/\theta_{offset}(^\circ)$	-1.0 / 0.0	0.0 / 0.5	0.2 / -1.0	1.0 / -1.0	-0.5 / 0.0
$\psi_{spin}/\psi_{offset}(^\circ)$	1.0 / 0.0	-0.8 / 0.0	1.0 / 0.0	-1.0 / 2.0	0.0 / 3.0
$\phi_{spin}/\phi_{offset}(^\circ)$	3.5 / 0.0	1.0 / 0.0	1.6 / 0.0	-0.8 / 0.0	10.5 / 0.0
u_{scale}	1.15	1.15	1.15	1.15	1.15
Time lag (s)	42	43	43	43	37
Time stretching (s)	1.0	1.0	1.0	1.0	1.0
R (m)	0.260	0.260	0.255	0.275	0.265

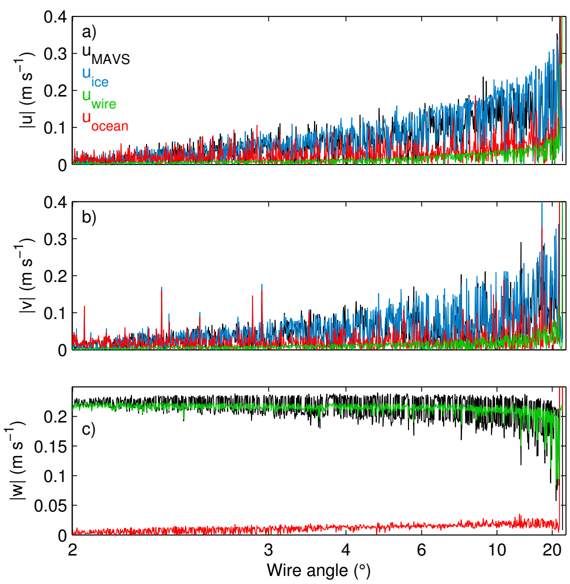

Fig. 5. Magnitude of ocean, MAVS, ice, and wire velocities vertically averaged from 8-250 m depth for ITP 78 sorted by average wire angle. a) eastward, b) northward, and c) vertical velocities. Fixed depth records are excluded. The magnitude of the angular velocity is small and not shown here.

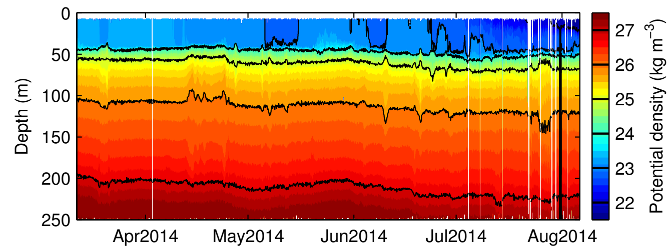

Fig. 6. Density versus time for ITP 78 in the upper 250 m. Eddies are evident as vertical spreading of density surfaces. Internal waves are evident as high frequency heaving of density surfaces.

and CTD sensors. Table I summarizes these parameters for each ITP-V system. The focus is on horizontal ocean velocity, since vertical velocity while profiling is more sensitive to the various sources of error (Sect. V). Two timescales, 4 s and 14 s, are used to minimize high-frequency noise. The choice of a 4 s timescale is explained in Section IV. The 14 s timescale arises from estimation of profiler attitude (Sect. III-B2), and is used for consistency in other parts of the processing. ITP 78 is used to illustrate the processing procedure since it has non-zero post-deployment calibration parameters as well as a range of wire angles. The upper 250 m observed by these ITP-Vs consists of a mixed layer that is around 40 m deep in winter and that shallows to less than 10 m in summer, strong stratification below the winter mixed layer base, and numerous eddies and internal waves (Fig. 6).

A. Pre-deployment calibration parameters

Each fully assembled ITP-V system is tested to determine biases in the accelerometer and magnetometer, as well as biases between the MAVS and IMU coordinate systems. The ITP-V is set in a jig (Fig. 2b) that is able to rotate the profiler through full 360° spins with reference measurements at fixed points of 15-30° spacing. The MAVS sting is the reference for the profiler orientation and so is aligned with magnetic north. Thus, any observed heading other than north indicates a misalignment between the MAVS and IMU sensors (and similarly for pitch and roll). The profiler is rotated in the north-south plane, and in the east west plane in 20° increments with sampling at each position for approximately 4 minutes (Fig. 7a). Magnetometer and accelerometer biases (Mx_{bias}, My_{bias}, Mz_{bias}, Ax_{bias}, Ay_{bias}, and Az_{bias}) are determined by independently fitting the magnetometer and accelerometer data to a sphere to deduce zero offsets. Misalignment between the MAVS sting and IMU sensors (θ_{spin}, ψ_{spin}, and ϕ_{spin}) is determined by rotating the spin test data by a series of bias angles until the data projects onto a pair of lines (e.g., Fig. 7b). These parameters are determined prior to deployment, and im-

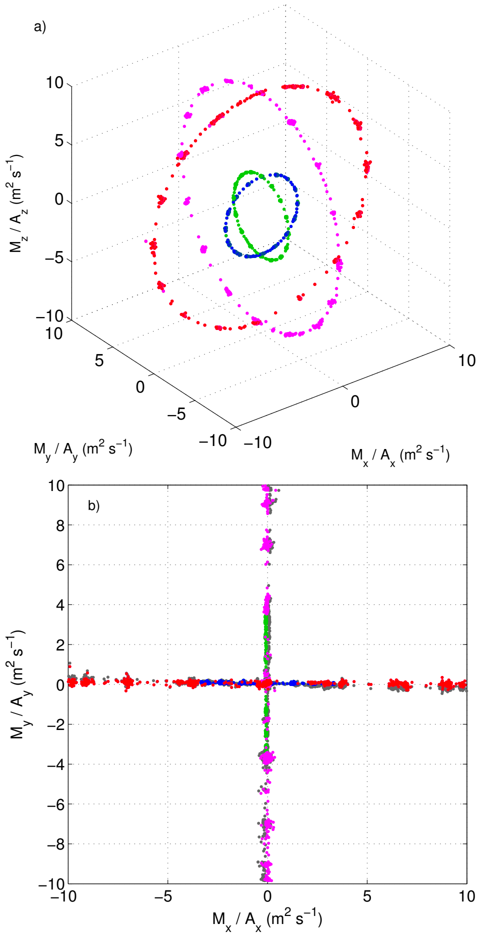

Fig. 7. ITP 77 spin test data for determination of pre-deployment calibration parameters. a) Magnetometer (blue and green) and accelerometer (red and magenta) data. b) Projection into the x-y plane without pre-deployment calibration parameters (gray) and with pre-deployment calibration parameters (color).

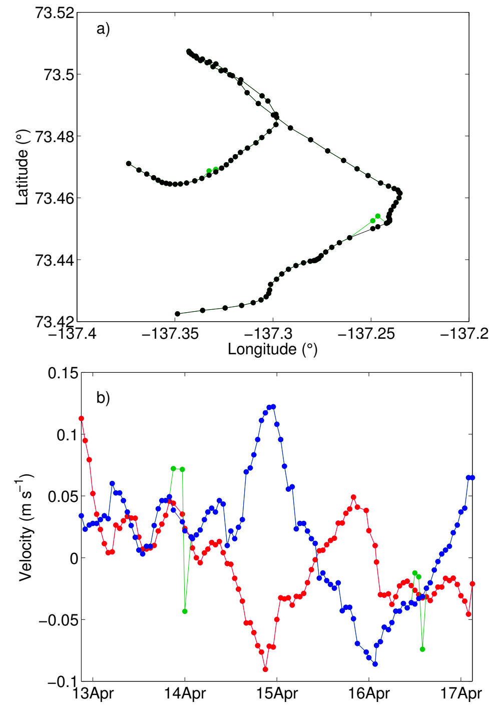

Fig. 8. Example GPS and velocity data over 4 days in April from ITP 77. a) Raw (green) and corrected (black) latitude and longitude. b) Raw (green) and corrected (blue) northward velocity. Eastward velocity is also shown (red).

plemented after data are telemetered to shore. Magnetometer and accelerometer biases ranged in magnitude from 0.007 to 0.326, and 0.001 to 0.719, respectively, which corresponds to less than a 10% bias (Table I). The largest accelerometer biases were in the vertical direction. Misalignment between the MAVS and IMU was less than 1° in magnitude for pitch and roll, and as large as 10.5° in magnitude for heading.

B. Derived quantities

1) Ice velocity: Ice velocity is determined from hourly GPS fixes of the surface buoy. In open water, this represents the speed at which the ITP translates horizontally through the water due to wind and currents acting on all parts of the ITP (it is still the relevant velocity in (1)). For these deployments, GPS position was taken at the top of the hour to synchronize position with co-located instruments; as the number of satellites visible is not always largest at the top of the hour, these ITP-Vs had more numerous degraded GPS fixes when compared with other ITPs. Bad latitudes and longitudes are flagged and replaced with corrected values. Values are flagged as bad based on spikes in the data that are inconsistent with typical ice motion, and manifest as a large positive velocity followed by a large negative velocity (Fig. 8). A threshold is initially used to flag bad points, and others are additionally flagged by hand. Corrected values are based on a quadratic fit to the nearest 4 good values. For the five ITP-V systems, 1-5% of the GPS data were flagged as bad by hand. Ice velocity was then linearly interpolated in time to the average time of each record.

2) Profiler pitch, roll, and heading: Pitch, roll, and heading of the MAVS are estimated from IMU data following [8]. Each estimate of pitch, roll, and heading employs a complimentary filter that combines a fast high-passed filtered estimate from telemetered IMU derived attitude estimates, with a slow low-pass filtered estimate from magnetometer and accelerometer data after biases are corrected for. Specifically:

$$\theta = f_{low}\left\{Tan^{-1}\left[\frac{Az + Az_{bias}}{-(Ax + Ax_{bias})}\right]\right\} + f_{high}\{\theta_{IMU}\} + \theta_{spin} + \theta_{offset} \quad (2a)$$

$$\psi = f_{low}\left\{Tan^{-1}\left[\frac{Az + Az_{bias}}{-(Ay + Ay_{bias})cos(\theta_{slow})}\right]\right\} + f_{high}\{\psi_{IMU}\} + \psi_{spin} + \psi_{offset} \quad (2b)$$

$$\phi = f_{low}\left\{Tan^{-1}\left[\frac{Bx}{-By}\right]\right\} + f_{high}\{\phi_{IMU}\} + \phi_{spin} + \phi_{offset} + declination \quad (2c)$$

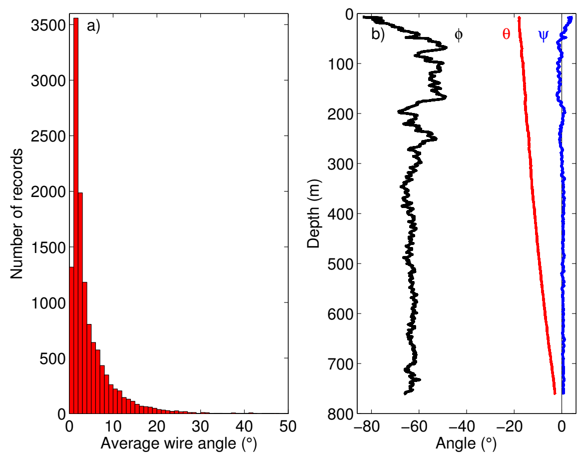

Fig. 9. a) Historgram of average wire angle in the upper 250 m for each record. Both profiles and fixed depth records are included. b) Example of pitch (red), roll (blue), and heading (black) from a 750 m profile (that shown in Figure 1b).

where spin angles are from pre-deployment calibrations (Sect. III-A), offset angles are from post-deployment calibrations (Sect. III-C), IMU angles are the angle estimates as telemetered by the IMU (based on the 200 Hz observations), f_{low} and f_{high} denote 14 s low-pass and high-pass filters, declination is the local magnetic declination, and Bx and By are the magnetometer observations ($Mx + Mx_{bias}$ and $My + My_{bias}$) rotated into the horizontal plane using pitch and roll. Wire angle is largest near the surface as the bottom weight forces the bottom of the wire towards vertical (e.g., Fig. 9b). Pitch, roll, and heading can change abruptly at the base of the mixed layer where shear tends to be large. Wire angle averaged over the upper 250 m was most commonly 1-2°, with 2% of wire angles in excess of 20° and occasionally reaching 40-50° (Fig. 9a).

3) Wire velocity: The velocity along the wire, $\mathbf{u_{wire}}$ is estimated from pressure and IMU data, and removed after MAVS velocity estimates are rotated into geographic coordinates. Specifically:

$$u_{wire} = \partial x/\partial t = \partial z/\partial t[tan(\theta)cos(\phi) + tan(\psi)sin(\phi)] \tag{3a}$$

$$v_{wire} = \partial y/\partial t = \partial z/\partial t[tan(\psi)cos(\phi) + tan(\theta)sin(\phi)] \tag{3b}$$

where $w_{wire} = \partial z/\partial t$ is derived from CTD pressure after smoothing with a 14 s low-pass filter. A 4-s low pass filter of CTD pressure introduces noise into fixed depth records and is not sufficient. Any vertical motion of the ice floe or ITP with periods longer than 14 s is accounted for in $\partial z/\partial t$ (and so w_{ice} is formally zero in (1)). Surface waves have periods of 10 s, and are not excluded, thereby contributing to uncertainties in w_{ocean}. The rotation by ϕ rotates from the heading aligned with the MAVS sting to geographic east and north.

4) Quality control: Five quality control flags are used to identify bad IMU and velocity values. These five flags are: accelerometer, angle rate gyro, and magnetometer have no signal ("1"), accelerometer and angle rate gyro are bad ("2"), the accelerometer is bad ("3"), the angle rate gyro is bad ("4"), and $\mathbf{u_{MAVS}}$ is bad ("5"). No signal corresponds to data having the same value for the entire record (either a profile or fixed depth record). Only 0.3% of data had no signal. Bad accelerometer (angle rate gyro) data corresponds to an accelerometer (angle rate gyro) magnitude, $Ax^2 + Ay^2 + Az^2$ ($Gx^2 + Gy^2 + Gz^2$), greater than 11 $m^2\ s^{-1}$ (0.8 $rad\ s^{-1}$). It may be possible to recover a signal from data with quality control flags of 2, 3, or 4, but due to the small number of points that are affected (0.6% of data), no attempt has currently been made. Bad velocity data corresponds to a velocity magnitude, $(u^2_{MAVS} + v^2_{MAVS} + w^2_{MAVS})^{1/2}$, greater than 0.6 $m\ s^{-1}$. This threshold is chosen so that large velocities associated with eddies are retained. Less than 0.1% of data had bad velocity signals, and most commonly occurred when the profiler was starting or stopping during a profile. Velocity data corresponding to these five flags are not used.

C. Post-deployment calibration parameters

Two of the post-deployment calibration parameters are associated with aligning the CTD and MAVS data in time as these sensors do not necessarily start sampling at the same time or sample at precisely the same rate. These parameters were implemented in the first ITP-V system, and described in [6]. Vertical velocity observed by the MAVS is compared with $\partial P/\partial t$ from the CTD to determine a single offset in time (time lag; Table I) and stretching factor (time stretching; Table I) for the entire deployment based on the start and stop signals from profiles (Fig. 4). All five ITP-Vs were found to have a stretching factor of 1.0 corresponding to sampling at the same rate, and an offset of 37 to 43 s (Table I). These calibration parameters are taken to be constant for all records of a given ITP-V.

Four of the calibration parameters (u_{scale}, θ_{offset}, ψ_{offset}, and ϕ_{offset}) are determined with the following procedure. Data with quality control flags of 1-5 (Sect. III-B4) are removed. Upward and downward profiles of velocity are independently plotted as a function of wire angle (Fig. 10). u_{scale} is set so that vertical velocity differences between upward and downward profiles are reduced. All five ITP-Vs had u_{scale} of 1.15, suggesting that the actual acoustic path is an arc that is somewhat longer than the shortest distance between transducer pairs. Pitch, roll, and heading offsets are determined by trying different values; an offset is chosen so that ocean velocity has as little dependence on wire angle as possible and the agreement between stationary and moving data as well as upward and downward profiles is good. If there is no discernible improvement over an offset of zero, an offset of zero is used. In most cases, it is only possible to determine angular offsets in 0.5° increments. Both the eastward and northward velocity components are considered in determining these parameters, with a mismatch of vertical velocity between upward and downward profiles being acceptable. Agreement between the first and last two minutes of the profiles when

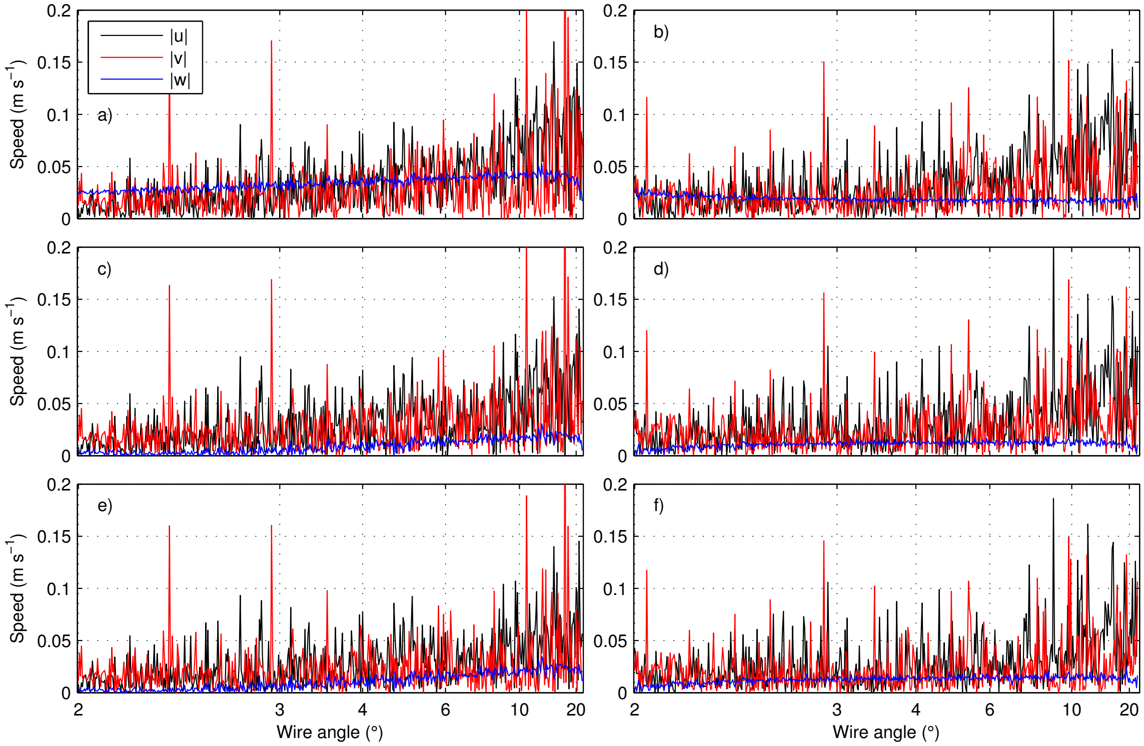

Fig. 10. Magnitude of ocean velocity vertically integrated over the upper 250 m a-b) without u_{scale} or angle offsets, c-d) without angle offsets, and e-f) with all calibration parameters. Upward profiles (a, c, and e) and downward profiles (b, d, and f) are shown separately. Results are similar when vertically integrated over depth ranges that exclude the mixed layer. Note that without u_{scale}, vertical velocities are of opposite sign for upward and downward profiles.

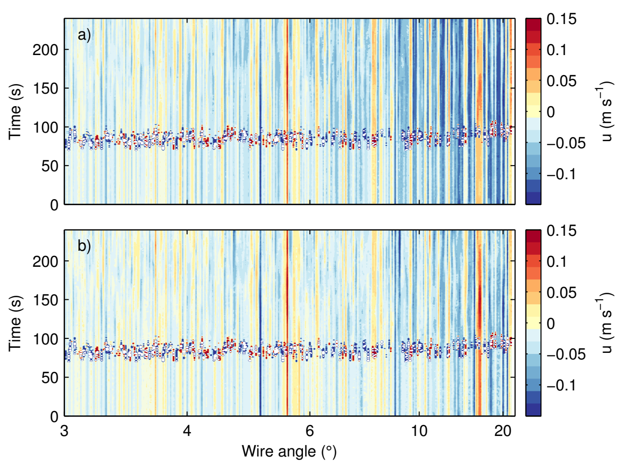

Fig. 11. Ocean velocity during the first 240 s of upward profiles a) without u_{scale} or angle offsets and b) with all calibration parameters. Only profiles with an average wire angle greater than 3° are shown. The profiler is stationary for the first 90 to 100 s, then rises from 250 m to approximately 215 m by 240 s.

the profiler is stationary is also considered (Fig. 11a), with greater emphasis on agreement at the bottom of profiles where ocean velocity does not change as rapidly with depth. It is primarily at higher wire angles, e.g., greater than 6°, where post-deployment parameters are most crucial (Fig. 11). The overall effect of u_{scale} and the offset angles is to reduce dependence on wire angle, improve the agreement between the stationary and profiling data, as well as the agreement between upward and downward profiles (Fig. 10, 11). As Table I shows, only 5 of the 15 possible angle offsets for the 5 ITP-Vs were found to be non-zero. The spin angles determined prior to deployment are most often all that is needed.

The final post-deployment calibration parameter is to determine an effective radius at which the MAVS sensor rotates about the wire. This is determined after the other parameters since it is small and primarily affects profiles at low wire angle. In coordinates aligned with the MAVS sensor, the angular velocity is only in the transverse direction, and is given by:

$$\hat{v}_{ang} = R * G_z \tag{4}$$

where R is the effective radius and G_z is the angle rate gyro measurement for rotation about the $\hat{z}$-axis that corresponds to velocity in the transverse direction. The term effective radius is used as it refers to the radius of the water sampled by the MAVS, which is larger than the radius at which the MAVS rotates about the wire. The effective radius is determined by finding the radius for which the variance of $\hat{v}_{ocean}$ is maximally smaller than the variance of $\hat{v}_{ocean} - \hat{v}_{ang}$ (Fig. 12a). The velocities are first smoothed with a 4 s low-pass filter to determine the effective radius (note that the angular velocity is not low-pass filtered in (1a)). Effective radii ranged from 25.5 to 27.5 cm, corresponding to a distance further from the wire than the MAVS as expected. After applying

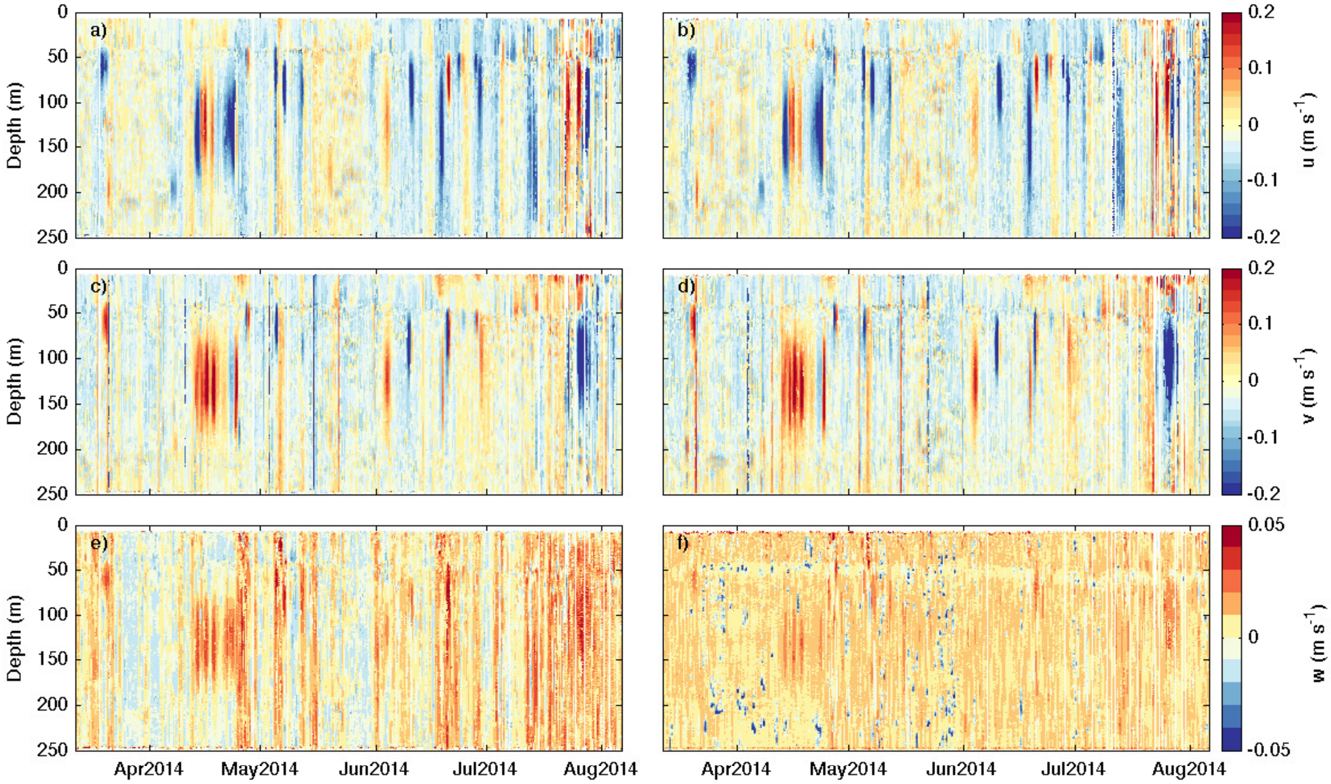

Fig. 13. ITP 78 a-b) eastward, c-d) northward, and e-f) vertical velocity binned in depth. Upward profiles (a, c, and e) and downward profiles (b, d, and f) are shown separately. Velocity shear is evident at the mixed layer base, due to eddies, and internal waves. The dark blue patches in downward vertical velocity (f) indicate where profiler wake effects are significant.

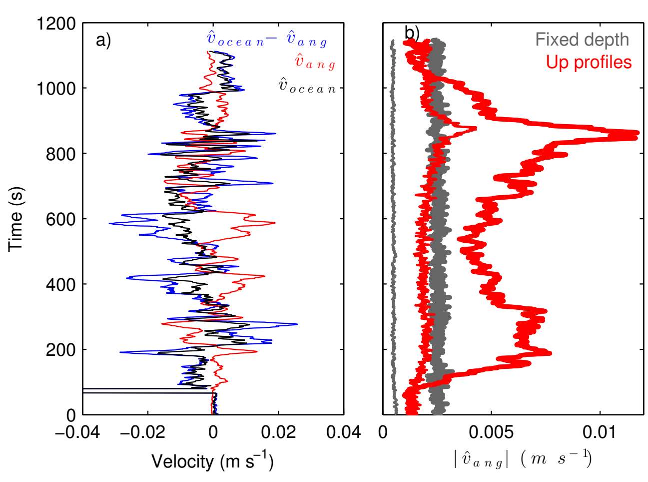

Fig. 12. Angular velocity due to rotation of the MAVS about the wire for ITP 78. a) $\hat{v}_{ang}$, $\hat{v}_{ocean}$, and $\hat{v}_{ocean} - \hat{v}_{ang}$ for record 165 (250 m up profile) with average wire angle of 3.5° and ice speed of 0.005 $m\ s^{-1}$, b) Average magnitude of the angular velocity for the largest (thick lines) and smallest (thin lines) 20% of up profiles (red) and fixed depth records (gray). The angular velocity for downward profiles is similar. All velocities are shown after a 4 s low-pass filter.

a 4 s low-pass filter, the angular velocity is at most order $0.01\ m\ s^{-1}$ for profile data, and $0.001\ m\ s^{-1}$ for fixed depth records (Fig. 12b). Large angular velocities while profiling result from a corkscrew motion of the profiler as it climbs the wire when no other flow is present, with upward and downward profiles rotating in opposite directions (not shown). Small misalignments of the fin with vertical, or how the wire passes through the curved rollers attached to the profiler could cause the corkscrew motion.

D. *Absolute ocean velocity*

Ocean velocity is estimated using (1) - (4). Profile data are binned to 1-dbar; fixed depth records are smoothed with a 4 s low-pass filter before fluxes are estimated (Sect. IV). The first and last 90 s of profile data where the profiler is stationary are removed prior to binning. Horizontal velocity for ITP 78 shows good agreement between upward and downward profiles with eddies and internal waves evident throughout the record (Fig. 13). Vertical shear of horizontal velocity (Fig. 14) shows that the one meter vertical resolution and careful processing of data are needed to examine the internal wave velocities found in the Arctic of order $0.01\ m\ s^{-1}$ or smaller. Derived ocean vertical velocity is also order $0.01\ m\ s^{-1}$, and is systematically biased between upward and downward profiles. While still subject to biases, vertical velocity from upward profiles shows dynamical signals associated with density features (see also Sect. V).

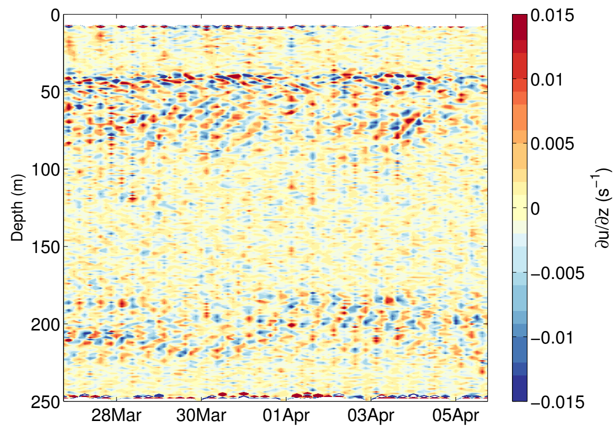

Fig. 14. Vertical shear of eastward velocity over a two week period at the end of March for ITP 78. Upward phase propagation corresponds to downward internal wave energy propagation.

IV. TURBULENT FLUX ESTIMATES

Vertical turbulent fluxes of heat, salt, and momentum are derived from fixed depth estimates using a direct correlation method. Example T, S, u, v, and w from a single 20 minute fixed depth record show some noise at the highest frequencies and correlations between variables at lower frequencies (Fig. 15a-b). Velocity spectra have a -5/3 power-law consistent with oceanic turbulence, and noise evident at periods less than 4 s (Fig. 15c). Fluxes are calculated as $\langle u'w' \rangle$, $\langle v'w' \rangle$, $\langle \theta'w' \rangle$, and $\langle S'w' \rangle$, where each variable is detrended and low-pass filtered at 4 s to eliminate this noise prior to averaging. The 4 second timescale is also consistent with the 4 s timescale associated with a 1 m vertical bin for profile data. Normalized cospectra of u and w show that the fixed depth records capture the dominant scales of turbulent fluctuations that have periods of several minutes. Spectra and cospectra involving T and S are similar and not shown. Turbulent fluxes low-passed filtered at 10 s are almost indistinguishable from those with a 4 s filter, indicating that high-frequency vertical ice velocity from surface waves can be reasonably neglected, and so the 4 s filter is used.

V. DISCUSSION OF ERROR

Errors arise from several sources, and impact quantities derived from observed velocity differently. One source of error is that associated with uncertainty in $\mathbf{u_{ice}}$ either through errors in GPS fixes or errors in linearly interpolating velocity derived from the 1 hour GPS record to the times of ITP-V records. Flux estimates from fixed depth records and velocity shear are not affected by uncertainties in $\mathbf{u_{ice}}$ since a mean is removed. Removing a mean similarly reduces errors from other sources as well.

Uncertainty in ocean velocity is also a function of wire angle to some extent. Wire angles that are large are more sensitive to errors in pitch, roll, and heading due to the increased influence of $\hat{w}_{wire}$ on horizontal velocity estimates. Wire angles close

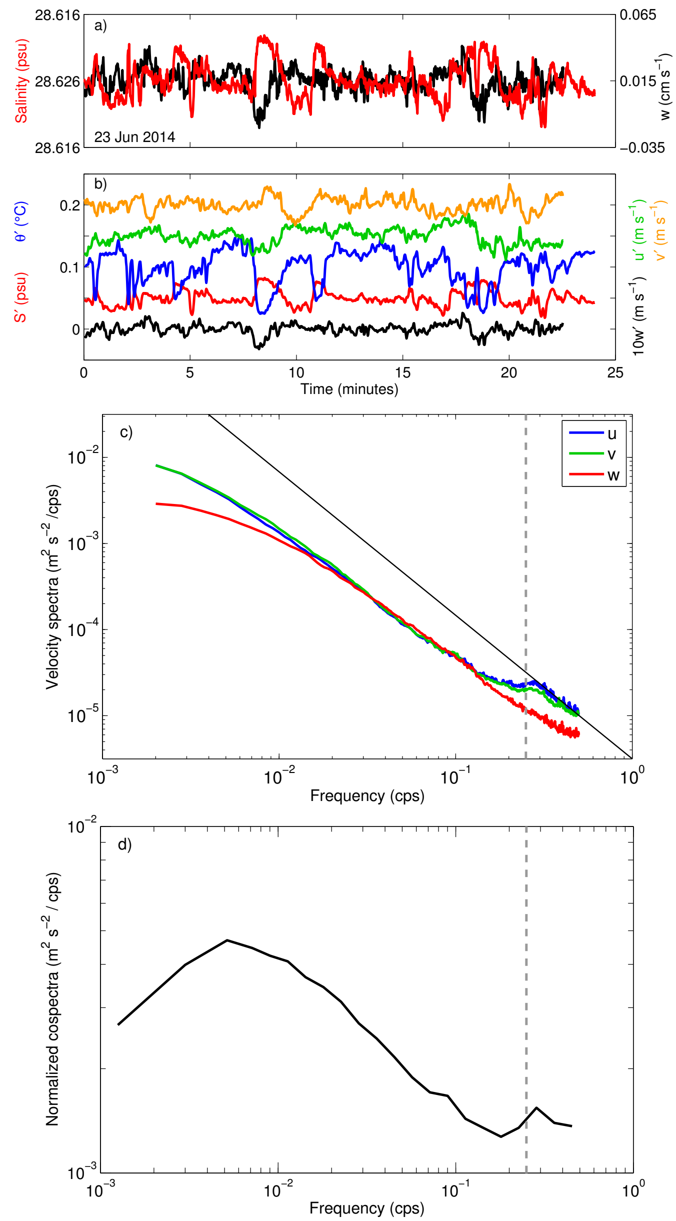

Fig. 15. Example data from a single fixed depth record from ITP 78 showing a) the 1Hz record, and b) the detrended and low-pass filtered records offset vertically. Pressure fluctuated between 8.26 and 8.30 dbar. Average c) velocity spectra and d) normalized cospectra of u and w from fixed depth records shallower than 15 dbar from all five ITP-Vs. The vertical dashed line shows a period of 4 s. Solid line in (c) has a slope of -5/3.

to zero are problematic due to profiler wake not being quickly advected away. At present, such wake effects are not removed or flagged, but are estimated to affect less than 1% of the data.

The processing procedures are derived with the goal of accurate horizontal velocity while profiling. During profiling, errors in pitch, roll, and heading will cause the motion of the profiler along the wire to be incorrectly accounted for and so result in errors in velocity. The combination of pre-deployment and post-deployment calibrations implemented here is done to minimize these errors as much as possible. Vertical velocity

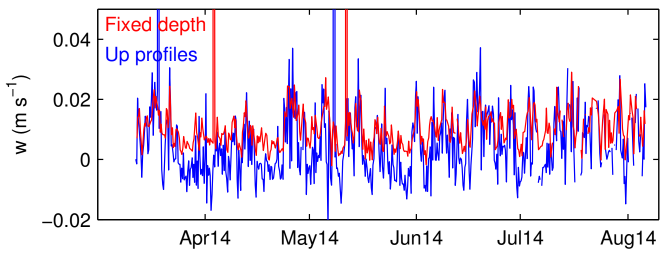

Fig. 16. Average vertical velocity for ITP 78 from upward profiles (red) and fixed depth records (blue) at depths less than 12 m.

while profiling is more sensitive to any such errors, and so biases remain. One test of the error in vertical velocity is to compare fixed depth velocities to velocities near the top of upward profiles. For all ITP-V systems, a bias of at most 0.01 $m\ s^{-1}$ is present, but the vertical velocities are well correlated over a range of frequencies indicating that the relative velocity signals where the mean vertical velocity over an ITP-V deployment is removed is more robust (Fig. 16).

Care has been taken in determining appropriate processing procedures at high frequency. Several dynamical quantities, including the vertical wavenumber spectra of velocity shear (not shown) and frequency spectra of fixed depth records (Fig. 15c), are checked to ensure that processing procedures are not introducing noise or otherwise masking relevant signals in ocean velocity. It is for this reason that processing sometimes includes high frequency signals (e.g., pitch, roll, and heading; Sect. III-B2) and sometimes excludes them (e.g., wire velocity is estimated from $\partial z/\partial t$ low pass filtered at 14 s; Sect. III-B3). Overall, the dynamically relevant velocity features with speeds of 0.01 $m\ s^{-1}$ or smaller suggest that errors in ocean velocity are tolerable.

The ability to determine the post-deployment processing parameters accurately depends in part on having a long enough record where there are profiles at both large and small wire angles. Small wire angles are essential to correctly determining the effective radius for the angular velocity, and large wire angles are essential to correctly determining post-deployment angle offsets. Shorter deployments of an ITP-V are possible, but to some extent will have velocity measurements subject to more uncertainty. The accuracy of real time current estimates similarly improves as the deployment lengthens. Some of the post-deployment parameters are similar between systems, e.g., u_{scale} and R, so that accurate real-time ocean velocity can be obtained with reduction in uncertainty as the deployment lengthens. The comparatively smaller number of 750 m profiles means that velocity processing relies on analysis of the 250 m profiles. These deeper profiles do improve post-processing of temperature and salinity.

VI. Summary

Ocean velocity as estimated from ITP-Vs is capable of resolving current features that are a) small in magnitude, b) have small temporal scales, and c) have small vertical scales. The combination of pre-deployment and post-deployment calibrations employed here ensures that biases affecting ocean velocity are as completely accounted for as possible. The careful treatment of high frequency signals ensures that averaging need only be done at a 4-s scale, and so preserves the 1-m vertical resolution of ITPs. Profiles and fixed depth records are processed identically. The simultaneous ability to observe both profiles of ocean T, S, u, and v (and to some extent w) together with vertical turbulent fluxes near the ice-ocean interface makes the ITP-V a powerful platform for understanding the ice-ocean system.

Acknowledgment

This work was funded by ONR grant number N00014-12-10140. Acquisition of the ITP-Vs was funded by DURIP grant number N00014-12-10799. We would like to thank Craig Marquette for his efforts in designing the pre-deployment spin test jig and implementing the spin tests. We gratefully acknowledge the support of the Beaufort Gyre Observing System and Joint Ocean Ice Studies (BGOS/JOIS) cruise on the *CCGS Louis S. St. Laurent* for deployment of ITP 70 and the recoveries of ITP 77 and 79. We would like to express our sincere thanks to the organizers and managers of the ONR Marginal Ice Zone camp operations including Larry Joireman, Jim Johnson, and Mike Carpenter, the crews of the Borek and B.A.S. Twin Otters, and Kris Newhall and John Kemp who's excellent efforts and professionalism made deployment of ITPs 77 through 79 possible. We also are indebted to the Korean Polar Research Institute (KOPRI) for allowing for the deployment of ITP 80 from the *RV Araon* and to Jeff Pietro for leading the deployment effort.

References

[1] Krishfield, R., J. Toole, A. Proshutinsky, and M.-L. Timmermans, 2008: *Automated Ice-Tethered Profilers for seawater observations under pack ice in all seasons.* J. Atmos. Oceanic Technol., 25, 2091-2105.

[2] Toole, J. M., M.-L. Timmermans, D. K. Perovich, R. A. Krishfield, A. Proshutinsky, and J. A. Richter-Menge, 2010: *Influences of the ocean surface mixed layer and thermohaline stratification on Arctic sea ice in the central Canada Basin.* J. Geophys. Res., 115, C10018, doi:10.1029/2009JC005660.

[3] Krishfield, R., J. Toole, and M.-L. Timmermans, 2008: *ITP data processing procedures.* Woods Hole Oceanographic Institution Tech Rep., 24 pp. [Available online at http://www.whoi.edu/fileserver.do?id=35803&pt=2&p=41486.]

[4] Thwaites, F. T., R. Krishfield, M.-L. Timmermans, J. M. Toole, and A. J. Williams, 2011: *Noise in Ice-Tethered Profiler and McLane Moored Profiler velocity measurements.* Proc. 2011 IEEE/EOS 10th Current, Waves, and Turbulence Measurements Workshop, Monterey, CA, IEEE Oceanic Engineering Society, doi:10.1109/CWTM.2011.5759553.

[5] Thwaites, F. T., R. Krishfield, 2013: *Development of a second-generation Ice Tethered Profiler with velocity sensor.* Proc. Oceans 2013 San Diego Conference, San Diego, CA, IEEE Xplore.

[6] Cole, S. T., M.-L. Timmermans, J. M. Toole, R. A. Krishfield, and F. T. Thwaites, 2014: *Ekman veering, internal waves, and turbulence observed under Arctic sea ice.* J. Phys. Oceanogr., 44, 1306-1328.

[7] Thwaties, F. T., and A. J. Williams, 1996: *Development of a Modular Acoustic Velocity Sensor*, Proc. OCEANS '96: Prospects for the 21st Century, 2, Fort Laurderdale, FL, MTS/IEEE, 607-612, doi:10.1109/OCEANS.1996.568296.

[8] Williams, A. J., F. T. Thwaites, A. T. Morrison, J. M. Toole, and R. Krishfield, 2010: *Motion tracking in an acoustic point-measurement current meter.* Proc. OCEANS 2010 IEEE, Sydney, Australia, IEEE, 1-8, doi:10.1109/OCEANSSYD.2010.5603862.